Adaptive Threshold and Weighted Frequency Domain Histogram of Local Binary Patterns

Tang Qi[1], Haixing Wang[2], Qunpo Liu[3]

[1,2,3] School of Electrical Engineering and Automation, Henan Polytechnic University, Jiaozuo, Henan, China

ABSTRACT: Wire ropes are crucial load-bearing components in mining conveyance equipment, and machine vision is one of the methods used to assess the surface damage condition of wire ropes. In response to the light-sensitive nature of local binary patterns, which leads to issues such as differing feature values for similar textures and susceptibility to the influence of excessively large or small pixels within local windows, hindering the accurate reflection of window structure information and exacerbating the introduction of considerable feature noise, an investigation is conducted. To enhance the gradient structural information among pixels within local pixel window, an adaptive threshold binary pattern feature operator is proposed. This operator utilizes the mean and variance within the local window to balance the central pixel value, thereby enhancing the interconnection among neighboring pixels. To perform feature selection on block histograms, a block-weighted approach is employed. This approach utilizes the concept of block weighting and employs correlation coefficients to preprocess feature vectors, thereby enhancing classification accuracy. The algorithm experiments were conducted on a dataset of mine wire ropes. The results indicate that the improved local binary pattern significantly enhances the classification accuracy of the wire rope dataset, achieving an accuracy of 97.3%.

KEYWORDS: LBP; SVM; Steel wire rope; Classification; Defect identification

I. INTRODUCTION

Wire ropes, as a key component of mine hoists, are subjected to vibration impact under the high speed and heavy loads of hoisting systems[1,2,3]. In mining operations, wire ropes are subjected to prolonged stretching, bending, and alternating loads[4,5], which inevitably produce defects and damage, such as broken wires, deformation, and missing strands; this damage increases greatly with time[6,7,8]. The high probability of safety accidents caused by wire rope damage poses a serious threat to the safety of operators and mining equipment and adversely affects the productivity of mining operations[9,10]. To ensure the efficiency of mining operations and to improve the reliability and safety of the equipment, a real-time wire rope damage detection system must be adopted in mining operations.

LBP and its derivative algorithms have exhibited some success in texture feature extraction. LBP is a powerful tool for describing the differential information within local boxes. It takes the center point as the threshold, quantizing the values of the surrounding neighboring pixels as "0" or "1" binary symbols, and composing the binary code using a certain order to express the distribution of pixels within the box. LBP is particularly sensitive to changes in illumination. When handling similar texture structures in an image, LBP and its improved algorithms lead to different coding values for similar structures under different conditions. This phenomenon seriously affects the performance of LBP and its improved algorithms in tasks such as classification and recognition.

Based on the above analysis, to enhance the gradient structural information among the pixels within the local neighborhood, an adaptive threshold binary pattern feature operator is proposed. This operator utilizes the mean and variance within the local neighborhood to balance the central pixel value, thereby strengthening the correlation among neighboring pixels. To perform feature selection on the block histogram, a weighted block approach is utilized, where the correlation coefficient is initially applied to process the feature vectors. This enables the learning of weights for each image block based on the concept of block weighting, ultimately enhancing the classification accuracy. To perform feature selection on the block histogram, a weighted block approach is utilized, where the correlation coefficient is initially applied to process the feature vectors. This enables the learning of weights for each image block based on the concept of block weighting, ultimately enhancing the classification accuracy.

II. LBP

The Local Binary Pattern (LBP) operator is a feature extraction method based on local image texture. LBP uses the grayscale value of the central pixel as a threshold to binarize the selected surrounding neighborhood pixel points. Specifically, if the grayscale value of a neighboring pixel point is greater than or equal to the grayscale value of the central pixel, it is labeled as 1; otherwise, it is labeled as 0. These binary labels are then combined in a clockwise manner to form a binary code. This

binary code is the LBP code value corresponding to each center pixel. Such as equation (1) and equation (2).

$$LBP_{r,p} = \sum_{p=0}^{p-1} s(x_{r,p} - x_c)2^p \qquad (1)$$

$$s(x) = \begin{cases} 1, & x \geq 0 \\ 0, & x < 0 \end{cases} \qquad (2)$$

III. LOCAL THRESHOLD BINARY PATTERN (LTBP)

The Local Binary Pattern (LBP) descriptor offers advantages in extracting texture structures. However, it suffers from issues such as limited structural diversity, weak noise resistance, and sensitivity to lighting conditions, which are particularly unfriendly for wire rope recognition in specific environments. The LBP descriptor quantifies neighboring pixels around a central pixel in a local window into "0" or "1" binary symbols, forming a binary code in a predetermined order to represent the distribution information within the window. Then, it calculates the weighted sum based on the quantized pixels. Therefore, LBP only focuses on the differential information between the central pixel and all neighboring pixels, neglecting the relationships between all pixels within the local window. As a result, it cannot fully represent the spatial structure of the image or address the introduction of noise.

To enhance the gradient information between pixels within the local window, this section introduces a strategy for updating the threshold TH for LBP thresholding. This threshold is related to the mean of the cumulative difference values $\bar{u}$ and the variance σ within the local window. The representation of the adaptive threshold local binary pattern is as follows:

$$ATLBP_{r,p} = \sum_{i=0}^{p-1} s(x_{r,i} - x_c)2^i \qquad (3)$$

$$s(x) = \begin{cases} 1, & x \geq TH \\ 0, & x < TH \end{cases} \qquad (4)$$

$$\bar{u}_{dif} = \frac{1}{p} \sum_{i=0}^{p-1} |x_{r,i} - x_c| \qquad (5)$$

$$\bar{u}_w = \frac{1}{p} \sum_{i=0}^{p-1} x_{r,i} \qquad (6)$$

$$\sigma = \sqrt{\sum_{i=0}^{p-1} (x_{r,i} - \bar{u}_w)^2} \qquad (7)$$

$$TH = \frac{1}{\sigma} \bar{u}_{dif} \qquad (8)$$

By introducing the average difference between the center pixel and its neighborhood pixels into the local binary pattern, the connection information between the center pixel and its neighborhood pixels is strengthened. Essentially, this expands the quantization range of the "0" or "1" binary symbols in the local binary pattern, effectively preventing noise introduction while preserving the rotational invariance of the LBP encoding.

Calculating the standard deviation of the pixels within the box is to evaluate the fluctuation of the pixels in the local box, measuring the flatness or steepness of the region. This is done to provide negative feedback to the average difference between the center pixel and its neighborhood pixels, preventing data offset caused by excessively large or small values in the average difference. This effectively prevents data sparsity and data coupling.

IV. WEIGHTED FREQUENCY DOMAIN HISTOGRAM

The LBP feature histogram reflects certain image structural information. Directly extracting the feature histogram of the entire image may lead to data coupling between image categories, resulting in the loss of a significant amount of information. Additionally, the positional characteristics of the LBP feature spectrum are completely ignored. This processing may result in irrelevant information inundating the image category features. To extract the main defects in the image and eliminate interference between different regions, the image is divided into blocks. Therefore, the LBP feature histogram divides the original image into non-overlapping regions and processes the LBP feature histogram for each sub-region. The feature vectors of each histogram are concatenated in a certain way to express the feature vector of an image.

Image segmentation allows for better understanding of the details in each block of the image, thereby providing a more detailed description of the overall image information, which is beneficial for subsequent defect recognition. Based on the aforementioned feature extraction methods, this chapter constructs a frequency histogram to effectively represent the features of the texture image. Such as equation (9).

$$H_i = \sum_{x,y} I\{f(x,y) = i\}, i = 0, \cdots, n-1 \qquad (9)$$

In the equation (9), n represents the feature values in the image.

$$I\{A\} = \begin{cases} 1, & A \ is \ true \\ 0, & A \ is \ false \end{cases} \qquad (10)$$

This histogram contains information about features such as edges and corner points. Considering the different defect positions on the steel rope, the feature histogram should include spatial information of the image. To achieve this, the image is divided into equal regions for histogram description, as shown in Equation (11).

$$H_{i,j} = \sum_{x,y} I\{f(x,y) = i\} I\{(x,y) \in R_j\},$$
$$i = 0, \cdots, n-1, j = 0, \cdots, m-1 \qquad (11)$$

In Equation (11), R_j represents different regions in the image. The segmentation histogram expression of the input image I is formed by concatenating the histograms computed for different regions, as shown in Equation (12).

$$H_{LBP} = \sum_{i,j} [H_{1,1}, \cdots, H_{i,j}] \qquad (12)$$

After studying and observing, it was found that the defective areas of the wire rope image are very small and irregularly shaped. These areas exhibit significant feature variations, while the normal regions occupy the majority of the image. Directly

using histograms with equal weights would directly affect the recognition results. Traditional histogram extraction ignores this characteristic. Therefore, constructing a weighted histogram feature is necessary, where the LBP histogram features containing defects are assigned larger weights. The principle of the weighted LBP histogram feature is shown in Equation (13).

$$H_{LBP} = \sum_{i,j} [w_1 H_{1,1}, \cdots, w_i H_{i,j}] \tag{13}$$

In Equation (13), w_i represents the weight of the feature histogram for each region.

The Pearson correlation coefficient is introduced in this paper to measure the correlation between the vectors of different image blocks. It is utilized for one-to-one or one-to-many partitioning into multiple groups, followed by weighting of the LBP features for each block.

The Pearson correlation coefficient is used to measure the degree of linear correlation between two continuous variables, primarily assessing the strength and direction of the linear relationship between the two variables. The formula is as follows:

$$\rho_{X,Y} = \frac{cov(X,Y)}{\sigma_X \sigma_Y} \tag{14}$$

In Equation (14): $\rho_{X,Y}$ represents the correlation coefficient between vectors X and Y, $cov(X,Y)$ represents the covariance between variables X and Y,, and X and Y represent the standard deviations of variables X and Y, respectively.

If an image is divided into N local regions, then the initialization of sample weights is as follows:

$$D^w = (w_1, w_2, \cdots, w_N), w_i = \frac{1}{n} \tag{15}$$

The equation indicates that D^w is a vector of weights for one image. When training weighted samples, the correlation vector for one block is obtained based on the joint correlation coefficient K:

Given that the defect type occupies a small portion of the image and assuming that the defect type is uncorrelated with other types, the values in the D_i^W vector tend to be generally small and relatively stable. The mean D_s in D_i^W is used as a criterion, and the following formula is employed to learn its weights.

$$\alpha_m = \eta ln \frac{1-D_s}{D_s} \tag{16}$$

here η represents the learning rate, and with the above formula, further weights for different regions in a single image can be obtained.

V. EXPERIMENT

A. Data Set

The data was captured using an industrial camera model MER2-2000-6GM under simulated lighting conditions similar to those in underground mines. These data were obtained from mining wire ropes under different operating conditions. The study involved wire ropes with diameters of 13mm for 810, 14mm for 619, and 22mm for 18*7. During the experiment, images were captured under simulated underground mining

conditions, successfully collecting images of four different defect types, including normal, missing wires, broken wires, and deformations. The dimensions of these images are 200 pixels by 400 pixels.
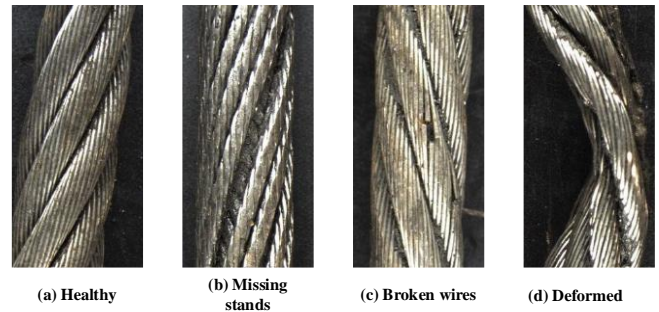

(a) Healthy   (b) Missing stands   (c) Broken wires   (d) Deformed

Fig1 Wire rope dataset

In the experiment, all texture images were first converted to grayscale images. Then, they underwent filtering and feature extraction processing. Subsequently, the images were partitioned into blocks, and the feature vectors were concatenated to form the feature vector of an image. Finally, normalization was performed. The dataset was classified in a "3:2" ratio for classification experiments. Additionally, the number of histogram features was uniformly mapped to the [0-15] interval. The experimental setup included a computer equipped with an Intel Core i5-7300HQ processor, 16GB of memory, and running on the Windows 10 operating system. The experiments were conducted using Python 3.7.

B. LBP Map

After encoding the images with LBP features, sorting them at the same positions in the images results in the LBP maps. LBP maps visually represent the magnitude and distribution of LBP values, aiding observation and analysis. Below are the LBP maps and improved LBP maps for comparative experiments under a 10*TH condition.
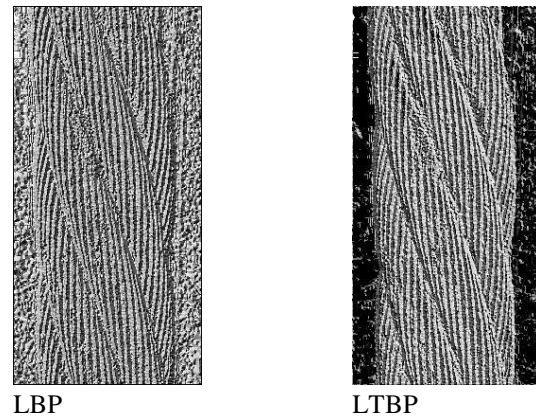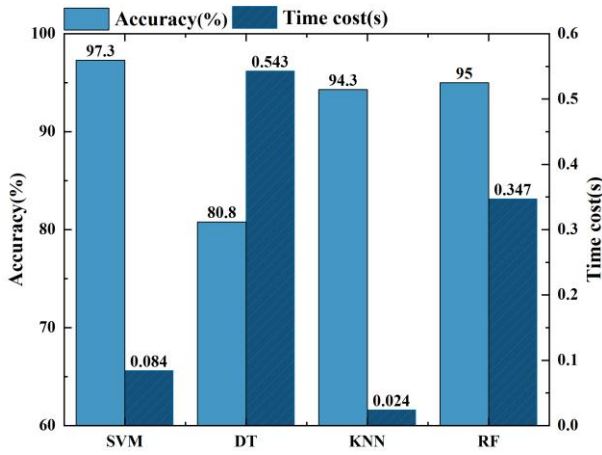

LBP   LTBP

Fig 2. LBP map

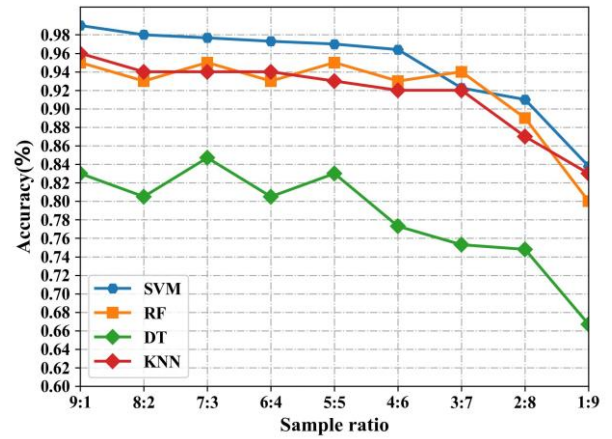**Fig 3. Comparison of accuracy between different classifiers**

Fig 4. Classification accuracy under different sample ratios

C. Classification Algorithm

Different machine learning classification algorithms have their own characteristics, and accordingly, they exhibit varying degrees of accuracy in recognizing surface defects in wire rope images. Therefore, this study examines the performance of extracted surface image features of wire ropes under three classification algorithms: SVM, KNN, and DT.

The experimental parameters for these four classification algorithms are set as follows: the maximum depth of the decision tree is 10, the minimum number of samples per node is 5, and the minimum samples per leaf node is 1; the optimal K for K-Nearest Neighbors algorithm is 1; the maximum number of decision trees for Random Forest is 100. The experimental results, as shown in Figure 4-12, indicate that the SVM classifier performs the best, with a multi-class precision of 97.3%, which is 16.3%, 3.3%, and 2.3% higher than DT, KNN, and RF, respectively. Moreover, in terms of algorithm execution time, SVM is only slightly higher than KNN, with 0.084s compared to 0.024s. The RF classifier exhibits slightly higher classification accuracy, but it consumes more than ten times the time compared to SVM. In this study, the SVM classifier was selected for defect recognition in steel wire ropes. As shown in Figure 4-13, the horizontal axis represents the ratio of training set to test set, indicating the classifier's classification accuracy under different ratios of training set to test set. It can be visually observed that SVM outperforms other classifiers in terms of classification accuracy. To comprehensively analyze the performance of the proposed feature operator, a training set to test set ratio of 3:2 was chosen.

D. Number Of Image Blocks

Image chunking can better grasp the detailed information of each piece of the image to obtain a more detailed description of the overall image information, which is conducive to subsequent defect recognition. The image is divided into n*n regions, and different sizes of region have a great impact on the recognition accuracy, feature extraction time and pattern recognition time.
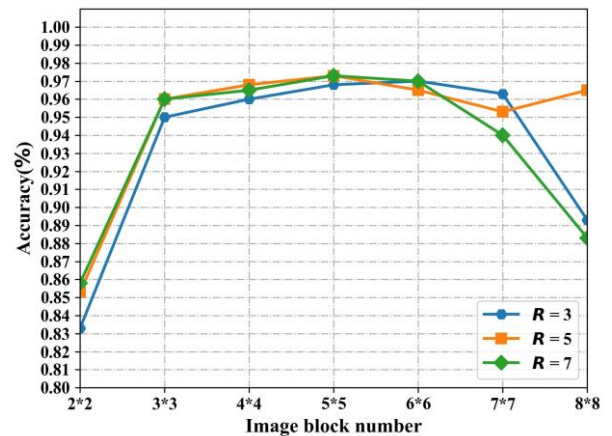

Fig 5. Recognition accuracy under different block numbers

The Figure 5 illustrates the performance of LBP features on the steel wire rope dataset with varying block sizes n*n. It shows that as the number of blocks increases, the classification performance of LBP features significantly improves under different filtering scales. This is because a larger number of blocks can extract more detailed texture structure information. However, as the number of blocks continues to increase, the classification performance of LBP features gradually stabilizes, with no significant improvement. This is due to the smoothing effect on defect feature histograms as the number of segmentation blocks increases, resulting in less distinct defect histogram distributions.
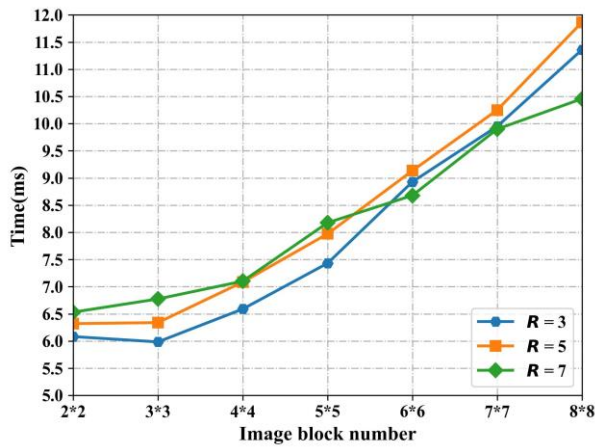
Fig 6. Recognition accuracy under different block numbers

Figure6 demonstrates the processing speed of exponential weighted guided filtering under different image block sizes and LBP sampling radii R. As the number of image blocks and the LBP sampling radius increase, the algorithm's processing speed also continuously rises.

E. LBP Parameters

TABLE 1. LTBP PERFORMANCE

r, p	Accuracy/%	$Macro-F1$	Time/s
$r = 1, p = 4$	0.88	0.8607	1.774
$r = 1, p = 8$	0.973	0.9652	3.103
$r = 2, p = 4$	0.863	0.8513	1.723
$r = 2, p = 8$	0.973	0.9654	2.968
$r = 3, p = 4$	0.825	0.8164	1.842
$r = 3, p = 8$	0.978	0.9633	2.952
$r = 3, p = 16$	0.915	0.9035	5.768

When the sampling radius increases, the classification accuracy of ARLBP feature vectors decreases. This is because as the sampling radius increases, the ARLBP feature vectors become more sparse, making it difficult to accurately estimate local image structures with similar local structural information, leading to a decrease in classification accuracy. However, with an increase in the number of sampling points, the classification accuracy of ARLBP features significantly increases. This is because extracting richer texture features leads to better performance.

The time consumption of the ARLBP feature extraction algorithm remains relatively unchanged with an increase in the sampling radius, while it significantly increases with an increase in the number of sampling points. Considering the overall performance of the ARLBP algorithm, it is recommended to choose LTBP features with $r = 1, p = 8$.

F. Comparison Of LBP Methods

To validate the effectiveness and superiority of the proposed local binary pattern features, experiments on classification accuracy were conducted using the steel wire rope dataset created in this study. The results were compared with several common texture feature extraction methods. These methods include Local Binary Pattern (LBP)[11], Non-Redundant Local Binary Pattern (NRLBP)[12], Extended Local Binary Pattern (Extended LBP)[13], Uniform Pattern Local Binary Pattern (UP-LBP)[14], Rotation Invariant Local Binary Pattern (RI-LBP)[15], Local Ternary Pattern (LTP)[16], Local Directional Pattern (LDP)[17], Local Optimal Pattern (LOP)[18], and Multi-Scale Local Binary Pattern (MB-LBP)[19].

This section compares and analyzes different texture feature extraction algorithms. The traditional LBP algorithm is highly sensitive to noise in image processing and lacks robustness to changes in the central pixel. The table shows that the proposed algorithm in this paper outperforms the above-mentioned algorithms and exhibits robustness to noise in the images. The table compares the feature extraction time and pattern recognition time of different algorithms. It can be observed that, except for Extended LBP, UP-LBP, and RI-LBP operators, the feature extraction time is significantly higher than that of other texture feature extraction algorithms. The LTBP algorithm proposed in this paper exhibits a moderate level of feature extraction time. From the table above, it can be concluded that LTBP is comparable to other algorithms in terms of feature extraction time and pattern recognition time, while achieving significantly higher recognition rates than other algorithms. Therefore, the proposed LTBP algorithm can provide excellent identification results for surface damage on steel ropes.

TABLE 2. THE RECOGNITION ACCURACY OF LBP ALGORITHM

Algorithm	Bins	Accuracy/%
LBP	256	86.02
Extended LBP	256	90.18
UP-LBP	59	89.70
RI-LBP	36	87.80
LTP	256	84.97
LDP	256	88.86
LOP	256	86.75
MB-LBP	256	89.01
NRLBP	128	83.65
ARLBP	256	97.3

VI. CONCLUSIONS

This paper addresses the complex and diverse textures, dispersed intra-class defects, and similar inter-class defects on the surface of steel wire ropes. It proposes an adaptive threshold local binary pattern (LBP) algorithm based on weighted frequency domain image blocks. Firstly, by partitioning the images, the overall detail information of the images is enhanced. Secondly, each image block is evaluated and its weight is learned using the joint correlation coefficient. Thirdly, the adaptive threshold LBP is employed to reduce the noise introduced by traditional algorithms and enhance the relationship between neighboring pixels, thereby improving the descriptive ability of the images. The experiments conducted on

the steel wire rope dataset demonstrate that the proposed algorithm significantly improves the defect recognition performance under the influence of both intra-class and inter-class features of the steel wire rope surface. The accuracy reaches 97.3%, addressing the issue of low recognition rates caused by insufficient texture description in traditional single-feature extraction methods.

REFERENCES

1. Liu Q, Song Y, Tang Q, et al. Wire rope defect identification based on ISCM-LBP and GLCM features[J]. The Visual Computer, 2023: 1-13.

2. Zhang Y, Cao G, Wang G. Vision-based measurement for the transverse-longitudinal-rotational displacement of hoisting rope by modified Lucas-Kanade algorithm[J]. IEEE Transactions on Instrumentation and Measurement, 2023.

3. Zhang Y, Cao G, Zhu Z, et al. Dynamic displacement measurement of hoisting rope in lateral and longitudinal direction by improving Lucas-Kanade algorithm[J]. Measurement, 2023: 113184.

4. Zhang N, Cao G, Zhu Z, et al. Nonlinear dynamics of time-varying curvature balance rope coupled with time-varying length hoisting rope in friction hoisting system[J]. Journal of Sound and Vibration, 2023, 567: 117910.

5. Chang X, Peng Y, Zhu Z, et al. Tribological behavior and mechanical properties of transmission wire rope bending over sheaves under different sliding conditions[J]. Wear, 2023, 514: 204582.

6. Tian J, Zhao C, Wang W, et al. Detection technology of mine wire rope based on radial magnetic vector with flexible printed circuit[J]. IEEE Transactions on Instrumentation and Measurement, 2021, 70: 1-10.

7. Li C, Wang D, Sun Y, et al. Bending fatigue damage behavior of wire rope in hoisting system of drilling rig[J]. Tribology International, 2023, 187: 108745.

8. Peng Y, Huang K, Ma C, et al. Friction and wear of multiple steel wires in a wire rope[J]. Friction, 2023, 11(5): 763-784.

9. Tytko A, Olszyna G, Kocór G, et al. Some Stochastic Aspects of Safety Work of Steel Wire Ropes Used in Mining-Shaft Hoists[J]. Sustainability, 2023, 15(9): 7590.

10. Siostrzonek T. The Mine Shaft Energy Storage System—Implementation Threats and Opportunities[J]. Energies, 2023, 16(15): 5615.

11. Ojala T, Pietikäinen M, Harwood D. A comparative study of texture measures with classification based on featured distributions[J]. Pattern recognition, 1996, 29(1): 51-59.

12. Nguyen D T, Zong Z, Ogunbona P, et al. Object detection using non-redundant local binary patterns[C]//2010 IEEE international conference on image processing. IEEE, 2010: 4609-4612.

13. Ahonen T, Hadid A, Pietikainen M. Face Recognition with Local Binary Patterns[M]. IEEE Computer Society, 2006.

14. Ojala T, Pietikainen M, Maenpaa T. Multiresolution gray-scale and rotation invariant texture classification with local binary patterns[J]. IEEE Transactions on pattern analysis and machine intelligence, 2002, 24(7): 971-987.

15. Pietikainen, M., T. Ojala and Z. Xu, Rotation-invariant texture classification using feature distributions[J]. Pattern Recognition, 2000.33(1): p.43-52.

16. Tan X, Triggs B. Enhanced Local Texture Feature Sets for Face Recognition Under Difficult Lighting Conditions[J]. IEEE Trans Image Process, 2010(6).

17. Jabid T, Kabir M H, Chae O. Gender Classification Using Local Directional Pattern (LDP)[J]. IEEE Computer Society, 2010.

18. T., C., et al., LOOP Descriptor: Local Optimal-Oriented Pattern[J]. IEEE Signal Processing Letters，2018.25(5): p.635-639.

19. Liao S, Zhu X, Lei Z, et al. Learning multi-scale block local binary patterns for face recognition [C]//Advances in Biometrics: International Conference, ICB 2007, Seoul, Korea, August 27-29, 2007. Proceedings. Springer Berlin Heidelberg, 2007: 828-837.